

# Investigation of Hybrid Power System for Marine Applications

T. SASILATHA<sup>1</sup>, D. LAKSHMI<sup>1</sup>, J. K. VAIJAYANTHIMALA<sup>1</sup>, R. K. PADMASHINI<sup>1</sup>, S. PRIYA<sup>1</sup>,  
J. PADMAPRIYA<sup>1</sup>, K. S. KAVITHA KUMARI<sup>2</sup>

<sup>1</sup>Department of EEE, AMET Deemed to be University, Chennai, Tamil Nadu, INDIA

<sup>2</sup>Department of EEE, Aarupadai Veedu Institute of Technology, Chennai, Tamil Nadu, INDIA

*Abstract* – Today's Marine industries are undergoing transformation because of rapid growth of advancement in the field of automation. Shipping industries use hybrid propulsion systems to de-carbonize and orient the path towards zero emission. The renewable energy supply (RES) is utilized by reducing the dependence on imported conventional fossil fuels; greenhouse gas emissions produced by the usage of fossil fuels are reduced. Renewable green energy is used to generate power at the distribution level. Energy sources are distributed around the world. The utility's hybrid (wind/solar) power system has proven to be a reliable source of energy. In this article, PV and wind (hybrid) power used for marine applications with the reduction of fuel consumption is proposed. The hybrid buck boost converter used for regulating DC output voltage. A multi-level H bridge inverter between DC-DC converter and load provides the load's ac voltage requirement in hybrid systems. For a given output waveform quality, MLI topology provide lower THD and EMI output, higher efficiency and better output waveform. In order to design a multilevel inverter, a cascaded H-Bridge structure was adopted. PWM (Pulse Width Modulation) techniques enable the operation of Cascaded H Bridges to generate an approximate sine wave output from a multilayer inverter. To improve the hybrid system's performance, output of converter is supplied to the thirteen level H bridge inverter. This combination can maintain the appropriate voltage to load ratio. Voltage profile is improved by using H-bridge multilevel inverter. The proposed framework is re-enacted utilizing MATLAB/Simulink.

*Key-words*— Hybrid power system, DC/DC converter, Solar PV system, WECS, multi-level inverter, on board ship, propeller, Total Harmonic Distortion.

Received: May 18, 2021. Revised: May 15, 2022. Accepted: June 18, 2022. Published: July 11, 2022.

## 1 Introduction

Issues over air quality and transport costs have inspired opportunities for future research in a variety of areas, primarily in the transportation industry. The naval and maritime sectors have taken massive steps to reduce airborne emissions and energy consumption around the world. The International Convention for the Prevention of Pollution from Ships organisation follows certain guidelines regulating pollution prevention and its effects on the marine environment [1].

Power generation of marine vessels has the capability to minimize fuel consumption and CO<sub>2</sub> emissions. The Integrated Power System integrates ship operations and electric propulsion into a single power platform, expelling the need for completely separate power generation for these loads. The Integrated Power System also has ON/OFF facility for alternative power resources, as well as the capacity to set up many such sources in a divided way, similar to a stand-alone micro grid, such as sustainability and energy storage systems (ESS). It

is now possible to enhance fuel economy and progress toward safer and more environmentally friendly marine vessels due to improvements in ESS technology. [2, 3]

In terms of fuel efficiency, hybrid onboard designs combined with ESS can either support or work in combination with DG to supply the load. As a result, depending on the DG usage period, operating costs can be reduced. [4] Explains the feasibility of an electric hybrid transportation vessel as a diesel-powered conversion. Investigation of SCES (Super capacitor energy system) and battery combination in ships for maximum power transfer is dealt in [5, 9]. In this regard, ESSs function as backup units that not only decrease the price of energising the system during peak demand and enhance the dynamic behaviour of the system, but could contribute to pollution reduction by removing unnecessary traditional unit commitment [10]. 190kwh battery prototype hybrid coastal fishing ship is demonstrated in [11].

Hybrid power system illuminates many key faults and challenges in hybrid RES design and development of energy management [12-14]. Environmentally friendly power sources, for example, Photovoltaic (PV) and wind turbine generators, which are powered by the sun, provide a viable alternative to motor-driven generators in such scenarios. [15-17].

The inherently unstable nature of wind and solar systems, as well as their reliance on weather, is a major disadvantage. To be completely reliable if used separately, most of these will need to be much larger, leading to a higher overall cost. Incorporating solar and wind energy into a hybrid power generation system, on the other hand, can reduce energy storage requirements while also lowering individual variability. [18-21]. the overall cost of the autonomous renewable system has been shown to be significantly reduced as a result of this structure [22-25].

In on board ships, integration of solar / wind systems with a battery bank and diesel backup is now a realistic and cost-effective solution.

Multilevel inverters incorporating some power semiconductor devices and DC voltage sources were also gaining popularity these days. [26] The most desirable topology is one with only one DC source. Recently, a five-level active-neutral-point-clamped system with an inductor and DC-link capacitor has been used. [27]. To provide power to the on-board ship, a multi-level inverter with 13 levels was implemented in this paper. Thus, the objectives of the proposed work are as follows.

To design a hybrid buck-boost converter and a 13-level inverter for the hybrid power system in order to maximise the use of renewable resources. The same model is verified using Matlab/Simulink. To select a optimal control mechanism for extraction of maximum power from RES system.

## 2 Configuration of Hybrid Power System

Figure 1 shows the configuration of Hybrid wind/PV system. This system consists of WECS /PV system for electric power generation with necessary MPPT controllers. The Buck-Boost Converter gets the variable output from the alternative sources, and the AC output from the multi-level inverter is used to power the ship's propeller.

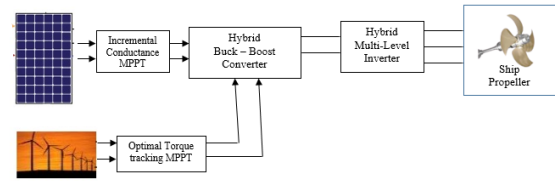


Fig. 1: Configuration of Hybrid Power System

### 2.1 Modelling of Solar Panel

Basic PV device is the configuration of PV modules. Entire PV generating unit is made up of this group of panels. A photovoltaic cell is a p-n junction semiconductor that converts light into electricity. To attain a specific voltage or current, single cells are connected in series or parallel to form a module. Figure 2 shows the equivalent circuit of PV cell.

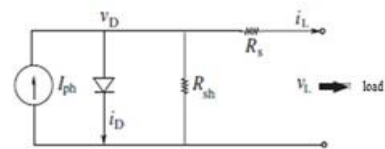


Fig. 2: Equivalent circuit of PV

Current source  $I_{ph}$  is the photocurrent of the cell.  $R_s$  and  $R_{sh}$  are the intrinsic series and shunt resistance of the cell. Group of PV cells are called as PV modules. Interconnection of modules in a parallel-series configuration is known as PV arrays. Equation (1), (2) and (3) represents the I-V characteristics of the solar panel

$$I = I_0 \left[ \exp \left( V + \frac{R_s I}{\alpha a V_t} \right) - 1 \right] - V + R_s I / R_p \quad (1)$$

$$V_t = N_s K T / q \quad (2)$$

$$I_i = N_{ph} I_{pha} \quad (3)$$

Where,  $I_{pha}$  is the current generated in a PV module,  $R_{se}$  and  $R_{sh}$  is the series and series resistance,  $I_d$  is the current of the Diode,  $V_d$  is voltage of the Diode,  $I_l$  is the current generated by Light in solar array,  $I_{pv}$  is the current of PV,  $I_0$  is current at saturation level,  $V_t$  is the thermal voltage of cells and  $A$  is the ideality factor of diode.

Moduled photo current of the PV is given in equation (4)

$$I_{pha} = [I_{scr} + K_j(T - 298)] * \lambda / 1000 \quad (4)$$

### 2.1.1 Maximum Power Point Tracking Methods

On the P-V curve, there is only one maximum voltage; it works at maximum power efficiency and delivers maximum output power. Maximum power point tracking (MPPT) controller act as a closed loop feedback system which senses PV output voltage and convert it into duty ratio for maximum power peak driving purpose. In non-linear solar P-V curves, the peak power point must be reached. some MPPT algorithms have been developed and utilized in some solid state devices.

#### 2.1.1.1 MPPT Techniques - INC

Due to its medium complexity and good tracking performance, the incremental conductance approach appears to be the most preferred. The MPP; however, magnitude generate oscillations around MPPs. The voltage at the array endpoints has always been set at MPP voltage. Oscillations are produced in the output power which is similar to P&O algorithm. Incremental conductance (dI/dV) of the photovoltaic array has been utilized in order to find the polarity of dP/dV.

Concept of hill climbing has been used in this INC method, in which the slope of P-V curve is zero at the point of MPP, negative at the right side of the curve and positive at the left side. It has been obtained by differentiating PV array power with respect to voltage and equating to zero and shown in Equation (5)

$$\frac{dp}{dv} = I + \frac{vdI}{dv} = 0 \quad (5)$$

When MPP is reached, then, the state would be like Equation (6);

$$\Delta I/\Delta V = -I/V \text{ at MPP} \quad (6)$$

MPP is achieved by comparing the incremental conductance with instantaneous conductance as shown in Equation (7),

$$\frac{\Delta I}{\Delta V} > -\frac{I}{V} \text{ to the left } \frac{\Delta I}{\Delta V} < -\frac{I}{V} \text{ the right of MPP} \quad (7)$$

Thus, the characteristic of INC compensates the disadvantages of P&O method. But in pracitcal, the constant point of Maximum value cannot be obtained. Hence there will be some oscillations near MPP.

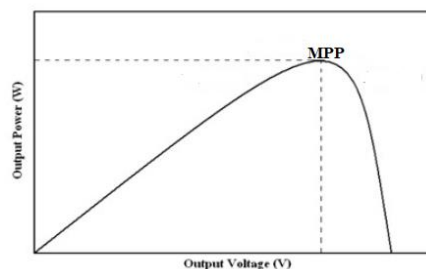


Fig. 3: MPP Tracking using INC algorithm

## 2.2 Modeling of a WT and Induction Generator

The most extensively used nonconventional, renewable energy source is wind energy. Wind Energy Conversion Systems (WECS) have seen tremendous technological improvement, which has resulted in a number of environmental, social, and economic benefits. Variable-speed WECS has a number of advantages over constant-speed WECS, including an increase in power production, a reduction in mechanical stress, and an improvement in power quality and system efficiency. Many Maximum Power Pointing Tracking (MPPT) strategies for variable speed operation of Wind Energy Conversion Systems have been developed in recent years to maximize power extraction.

### 2.2.1 Optimal Torque Control

Optimal torque management can also be used to achieve maximum power output, as shown in Equation (9);

$$T_M \propto \omega_M \quad (9)$$

The mechanical torque of the turbine is  $T_M$ , while the turbine speed is  $M$ . Because the mechanical power losses of the gearbox and drive train are ignored for a given gear ratio, the turbine mechanical torque  $T_m$  and speed  $\omega_M$  are identical to the generator mechanical torque  $T_m$  and speed  $\omega_M$ . The desired torque reference  $T_m$  is calculated using the generator speed  $w_M$ . The coefficient for the optimal torque  $K_{opt}$  can be derived using Equations (10) to (13) based on the generator's rated characteristics.

$$P_{max} = C_{p,opt} * \omega^3 \quad (10)$$

$$K_{opt} = \frac{1}{2} \rho C_{p,opt} \pi \frac{R^5}{\lambda_{opt}^3} \quad (11)$$

$$C_{p,opt} = \frac{1}{2} \left( \frac{116}{\lambda_i} - 0.4\beta - 5 \right) e^{-\frac{21}{\lambda_i}} \quad (12)$$

$$\frac{1}{\lambda_i} = \frac{1}{\lambda_i + 0.08\beta} - \frac{0.035}{\beta^3 + 1} \quad (13)$$

Wind, being one of the most widely used renewable energy sources, appears to have the best chance of replacing fossil fuels in the near future. Maximum power point tracking (MPPT) in variable-speed operating systems, such as doubly fed induction generator (DFIG) and permanent magnet synchronous generator systems, has received a lot of attention in order to achieve high efficiency in a wind power conversion system. Three tactics have been investigated throughout the history of MPPT methods: use wind speed; output power measurement and calculation and the characteristic power curve.

The majority of wind energy control systems rely on wind speed measurements. Anemometers are commonly used in these systems to measure wind speed. Sensor costs and complexity add to the cost of such systems. Wind speed estimating methods were employed to solve this challenge. The wind speed can be recorded using advanced software techniques in order to control the appropriate tip-speed ratio and perform the MPPT. Additionally, tracking the maximum power could be done by directly measuring the output power. The goal of this method is to extract maximum power from the wind turbine system by measuring output power online and checking the rate of change of power with regard to speed, i.e.,  $dp/dw$ . When  $dp/dw=0$ , MPPT can be performed by altering the rotor speed or duty cycle of the converter.

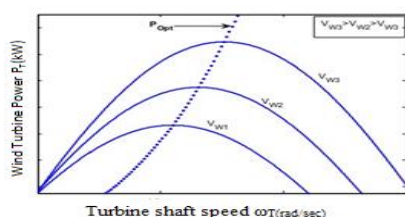


Fig. 4: Wind turbine power curves

### 2.3 Hybrid Buck – Boost Converter

The circuit diagram of buck-boost converter is shown in figure 5. The variable output of RES is fed into a Diode Bridge with an inductor and capacitor across the load. Energy is stored in the inductor during ON of switch and discharged when in OFF state therefore the converter can be used as a step-down or step-up converter. By switching the switching device appropriately, the voltage can be boosted or dropped. Duty cycle regulates the output voltage. By appropriately adjusting the switching

device, voltage can be boosted or reduced. The output voltage is determined by duty cycle. The circuit is conducted in two phases here. The Diode Bridge circuit conducts the rectification process, the IGBT switch performs the switching, and the PWM approach is utilized for output voltage control.

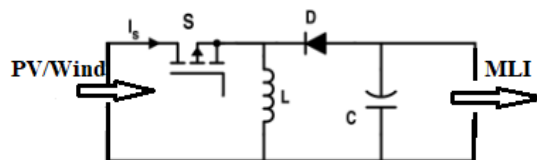


Fig. 5: Circuit Diagram of Hybrid Buck-Boost Converter

### 2.4 CHBI (Cascaded H Bridge Multilevel Inverter)

Cascaded inverter is dependent on DC sources. For  $m$  DC sources, the levels should be  $(2m+1)$ . The CHB inverter can be categorized as symmetric or asymmetric depending on the input level. The asymmetric topology is considered in this paper. To generate thirteen-level output, six asymmetrical DC sources are used. By using this network, the number of switches and THD are reduced. Figure 6 shows the thirteen level Inverter considered.

#### 2.4.1 Modelling of CHBI

The output voltage for full bridge inverter is given by Equation (13)

$$V_{oj} = V_{dc}(S1j - S2j) \quad (13)$$

For input DC current by Equation (14);

$$I_{dcj} = I_a(S1j - S2j) \quad (14)$$

Where  $j=1,2,3, \dots, n$

$I_a$  is the cascaded inverter output current,  $S_{1i}$  and  $S_{2i}$  are the switches of bridge circuit. The output voltage/phase is given by Equation (15)

$$V_{on} = \sum V_{oj} \quad (15)$$

where  $j=1,2,3, \dots, 6$

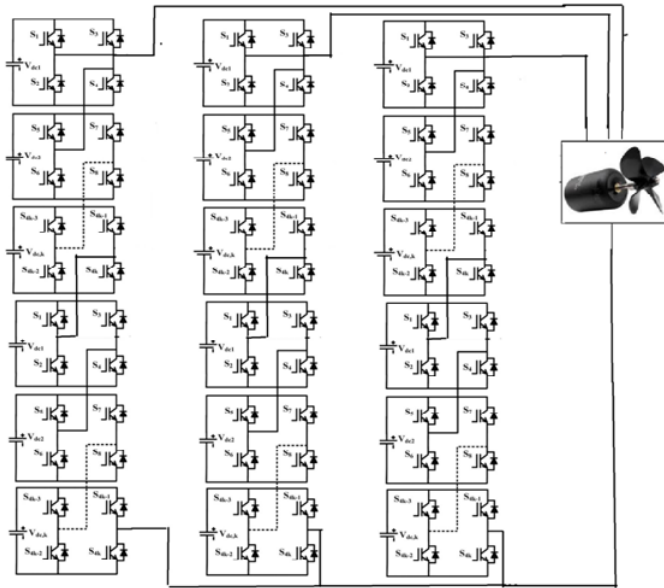


Fig. 6: Structure of thirteen level Inverter

### 3 Simulation results and Discussion

#### Case (i) Solar PV fed MPPT Controller based Buck Boost Converter:

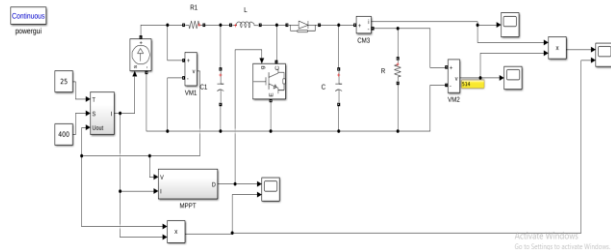


Fig. 7: Simulation of Photovoltaic buck Boost converter with MPPT controller

To do this, a MATLAB/Simulink simulation is being used to show the suggested system's concert. PV cell is employed as the input source, with an isolation level of 1000 Watts per square metre. The PV cell's output voltage is 24V PV (photovoltaic), which is fed through a buck boost converter to produce a voltage of 415 V, which is used to power a 1 HP induction motor coupled propeller. This experiment used a 50 mH inductor and a 1 mF capacitor. Figure 7 shows a simulation diagram of PV with MPPT.

The PV panel's unregulated dc output is adjusted using a Buck-boost converter. The switching device used is an IGBT. The duty cycle is determined by comparing the MPPT algorithm output to a carrier wave. DC-DC chopper converters that drop and increase voltage are known as buck-boost converters.

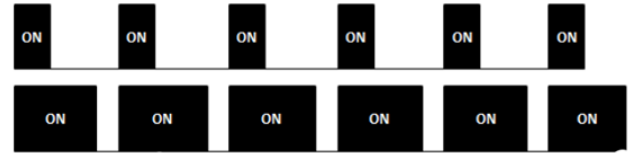


Fig. 8: Buck Boost operation using PWM control

When the volt produced is altered, the duty factor changes in the INC method; when the voltage is reduced, the PWM's threshold voltage rises. When the voltage exceeds the threshold, the PWM is engaged, and the buck converter with a 20% PWM "ON" duration and a buck converter with a buck spends 80% of the time "OFF." When the output does not match the input, something occurs.

When the voltage output is less than the threshold value, boost converter's PWM wave will be in ON state for 80 percent and an OFF time of 20 percent. Depending on the voltage variation at the output, the duty cycle is set between ten percent and ninety percent. This is depicted in Figure 8.

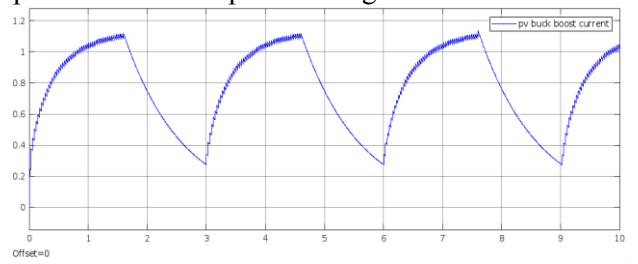


Fig. 9: Simulation of Photovoltaic buck Boost converter current output

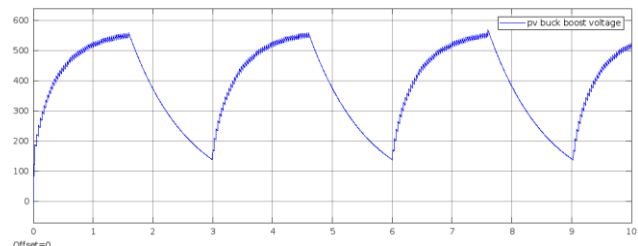


Fig. 10: Simulation of Photovoltaic buck Boost converter voltage output

Figure 9 and 10 displays the output current and voltage of a Buck boost converter. The propeller cannot be driven with these outputs. This converter's dc output should be fed into a multilevel inverter to generate AC output.

Because solar irradiance and temperature change over time, MPPT controllers are used to extract maximum power and create a satisfactory output.. The output of the solar cell is then directed into a dc / dc converter. The duty cycle can be adjusted to provide the desired output. Any method can be used to generate the switching frequency for the buck boost converter.

In this scenario, the INC method is used. The INC technique is depicted in Figure 11 as a simulation graphic. Changing the voltage and then measuring the power yield is part of the Incremental conductance algorithm. When the movement is on the left side of the MPP, voltage incrementing causes the option to boost, and when the movement is on the right side of the MPP, it causes the power to drop.

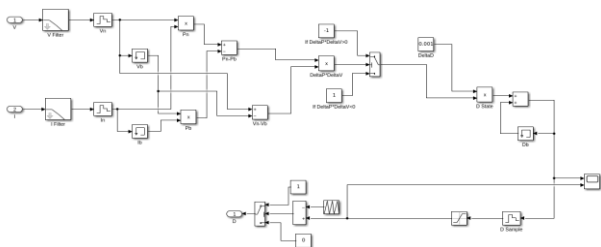


Fig. 11: Simulation diagram of Photovoltaic mppt controller

Through using output current ( $i_{pvCk}$ ) and output voltage ( $V_{pvCk}$ ) from the PV module's output terminal, this algorithm calculates the output power ( $P_{pvCk}$ ). The output power ( $P_{pvCk}$ ) will be compared to the final step of power computation ( $P_{pvCk-1}$ ) to determine the maximum power point; the difference between the two figures will be zero. If the difference is not zero, the next stage of computation will analyze the ( $V_{pvCk}$ ) and ( $V_{pvCk-1}$ ) values to indicate the direction of the power point on the RHS or LHS of the P- V curve Figure 12. ( $V_{pvCk-1}$ ).

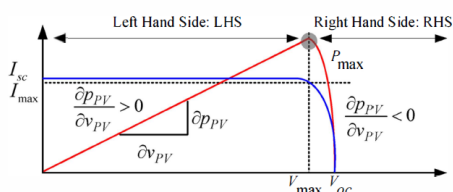


Fig. 12: PV module I- V and P- V curves, as well as maximum power point

By comparing old and new data, the duty cycle is computed. In the diagram below, the enhanced MPPT controller power is also depicted.

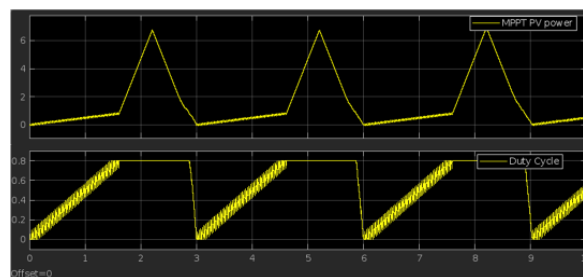


Fig. 13: Simulation output of power and duty cycle from a MPPT Controller

### Case (ii) Wind Energy fed MPPT Controller based DC-DC Converter

WIND GENERATORS (WGs) have been widely employed to power remote loads in both autonomous and grid-connected applications. Although WGs are less expensive to install than photovoltaics, the overall cost of the system can be further reduced by utilising high-efficiency power converters that are tuned to provide the best output based on current atmospheric conditions. The blade pitch angle can be mechanically changed to control WG power generation [6]. On the other hand, special-purpose WGs are frequently required, particularly in small-scale stand-alone WG systems. Figure 14 is a simulation figure depicting the power characteristics of wind turbines.

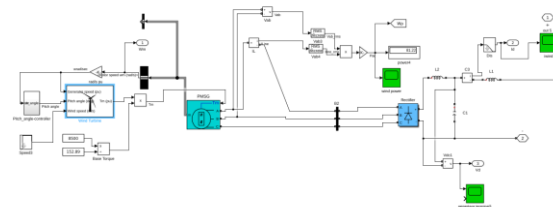


Fig. 14: Wind turbine power characteristics simulation

The WG load is modified, resulting in a variable-speed WG operation that captures maximum wind power on a continual basis (MPPT control). Another benefit of variable-speed operation is that as the WG rotation speed changes, the blades absorb the wind torque peaks, decreasing stress on the WG shafts and gears. Variable-speed operation has the drawback of necessitating the usage of a power conditioner in order to simulate the WG perceived load. On the other hand, advances in power electronics have helped to lower the cost of power converters and enhance their dependability, while the higher cost is offset by increasing energy generation.

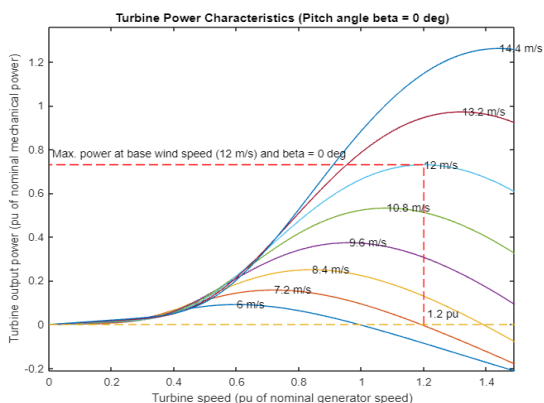


Fig. 15: Wind Generator power curves at various wind speeds

A control system based on wind-speed readings [7] is shown in Figure 15. After the wind speed is measured, the required rotor speed for maximum power generation is computed. Furthermore, the rotor speed is measured and compared to the determined optimal rotor speed, with the difference being used to run a power interface. Using measurements of the Wind Generator output voltage and current, the MPPT technique monitors the Wind Generator output power and adjusts the dc/dc converter duty cycle instantly based on a comparison of sequential Wind Generator -output power data. Based on a comparison of consecutive Wind Generator -output-power measurements, the MPPT technique in the proposed system changes the duty cycle of the dc/dc converter immediately. Despite the wide range of wind speeds, the power received by the Wind Generator varies very slowly over time because to the linked wind-turbine/generator system's poor dynamic response.. As a result, the steepest ascent strategy may be able to successfully address the challenge of improving Wind Generator output power by utilizing the converter operating frequency as a control variable.

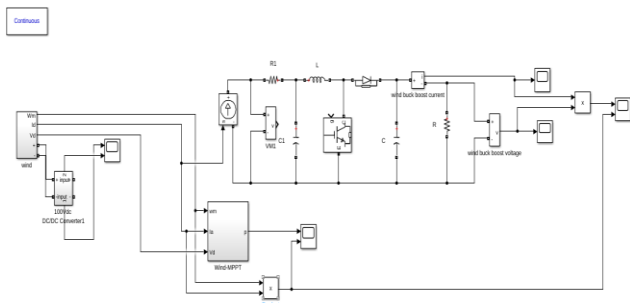


Fig. 16: Simulation of wind energy conversion using a buck boost converter and an MPPT controller

To increase smoothing and constant output performance, a PMSG is utilised to provide

changing frequency and voltage at the output, which is then fed into the Buck-Boost converter. For research purposes, a simulation of this topology was done in MATLAB/ Simulink. A Simulink model of a PMSG supplying a resistive load via a Buck-Boost converter is shown in Figure 16. With a fixed dc or inverter output, the Buck-Boost converter uses a PWM regulating technique to provide three phase balanced output voltage and frequency.

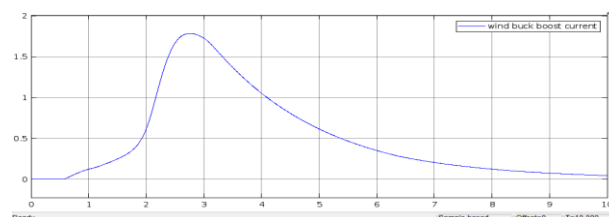


Fig. 17: Wind Energy BUCK BOOST Current Simulation Result

Regardless of the type of generator utilised, the accuracy with which the peak power points are tracked by the WECS control system's MPPT controller determines the amount of power produced by a WECS. The three main control approaches investigated so far in maximum power extraction algorithms are tip speed ratio (TSR) control, power signal feedback (PSF) control, and hill-climb search (HCS) control [8]. The method used by the P&O algorithm is to use a mathematical optimization strategy to locate the MPP. Changing control factors such as the dc-link voltage or the rotor speed and seeing how they effect WECS performance is part of this strategy. In the classic P&O (CPO) technique, the obtained power is combined with the generator speed to get a zero slope for the P-curve. The key features and advantages of this method are that it does not require any sensors, such as an anemometer, or knowledge of the WT parameters.

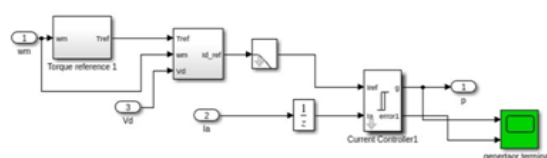


Fig. 18: MPPT Control block in WECS

The controller adjusts the operational point of the CPO algorithm to the right of the MPP if it is to the left of the MPP, and vice versa[9-10]. Using information on the size and direction of change in power output owing to a change in command speed, the MPPT controller calculates the ideal speed for maximum power point.

The operation of the controller is described below. If the difference between current and past sampling instants  $P_0(k)$  is within a given lower and upper power limit PL and PM, no action is done; however, if it is outside this range, appropriate control action is taken. The magnitude and direction of the change in active power caused by the change in command speed dictate the control action.

- If the power in the current sampling instant is higher, i.e.  $P_0(k) > 0$ , the command speed is raised, either due to an increase in command speed or because the command speed was unaltered in the prior sampling instant, i.e.  $(K-1) \geq 0$ .
- If the power in the current sampling instant is determined to be higher, i.e.  $P_0(k) > 0$ , the command speed is reduced due to a decrease in command speed in the preceding sampling instant, i.e.  $(K-1) < 0$ .
- In addition, the command speed is reduced if the power in the current sampling instant is discovered to be lower, either due to a constant or greater command speed in the prior sampling instant, i.e.  $(K-1) \geq 0$ .
- Finally, if the current sampling instant's power is found to be lower, i.e.  $P_0(k) < 0$ , because the prior sampling instant's command speed was lower, i.e.  $(K-1) < 0$ , the command speed is increased.

The product of the magnitude of power error  $P_k$  and  $C$  determines the size of each change in command speed in a control cycle. The value  $C$  is determined by the wind speed. During the maximum power point tracking control operation, the above-mentioned product gradually lowers until it reaches zero at the peak power point.

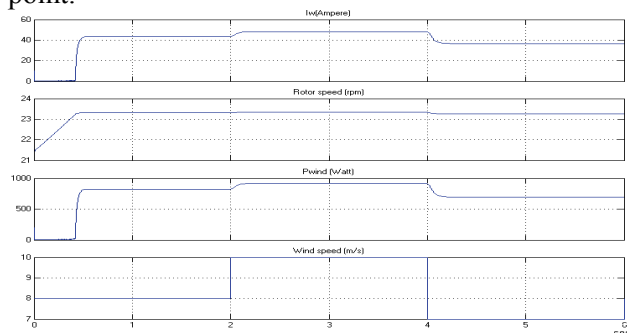


Fig. 19: Shows the results of a simulation of a wind energy system controlled by MPPT

To test the performance of the recommended controller, a rectangular speed profile with a maximum of 9 m/s and a minimum of 7 m/s was applied to the PMSG WECS. Figure 19 shows the wind speed, rotor speed, power coefficient, and active power output for this sample. The tracking

capability was found to be exceptional. The highest CP value for the turbine studied was 0.48, while the lowest CP value was 0.33, suggesting that the proposed controller functioned effectively. It is reasonable to conclude from the simulation results that the suggested control algorithm can track peak power locations. The method could be applied to other types of WECS as well.

**Case (iii)**  
**Solar/Wind Fed Multilevel inverter fed Induction motor driven propeller**

The Induction motor driven propeller integrated with a hybrid PV/wind-based power system, designed and managed by the P&O MPPT algorithm, has been described in this section. Figure 20 depicts the detailed simulation model.

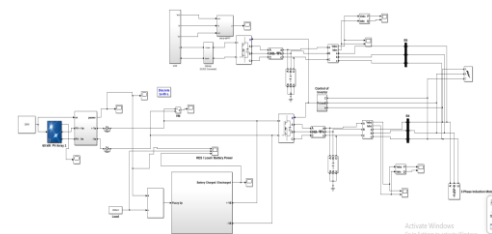


Fig. 20: Simulation result of wind energy system with MPPT control

The outputs of the solar photovoltaic system with MPPT controller are tested individually. The P&O MPPT controller is accounted for. Because of the ease with which the P&O system can be developed. Despite variations in insolation, the duty cycle of the buck boost converter is controlled to provide the regulated DC output from the Photo voltaic cell. A hybrid energy system with variable speed wind generation and a solar system with a power electronic interface was described in this paper in stand-alone mode. MATLAB/SIMULINK was used to run the computer simulation. The system's performance was examined for various wind speeds and irradiation levels in the stand-alone mode, and the results were analysed. AC voltage varies due to differences in wind speed and sun irradiation. The battery system is utilised to keep the source and load in balance. In the MATLAB/SIMULINK platform, the performance of the developed system with proposed Induction Motor driving parameters of current, speed, and torque can be tested, and the results are shown.

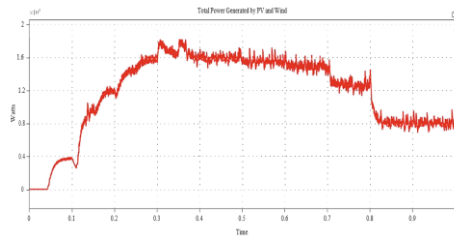


Fig. 21: Output power of hybrid PV/wind energy system

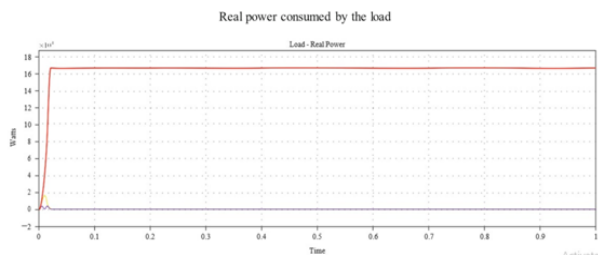


Fig. 22: Load's actual power consumption

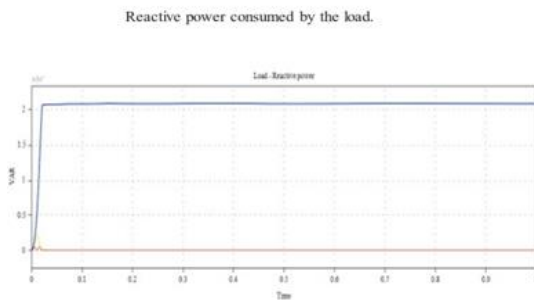


Fig. 23: Load's reactive power consumption

Both the PV cell and Wind Energy outputs are fed through a nine-level inverter, which generates input for a three-phase induction motor. The modulation technique employed is phase shift modulation, which reduces THD levels.

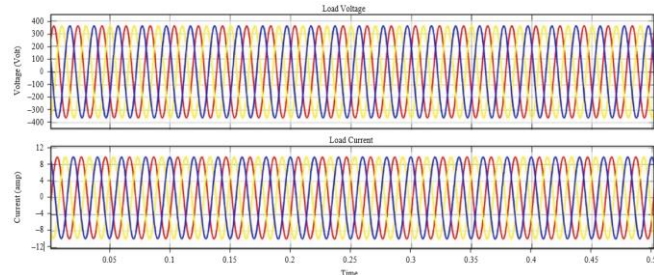


Fig. 24: Output current and voltage

By adjusting the modulation index  $m_i$  by varying the carrier and the reference frequency the output voltage and current are obtained and is given as input to the induction motor to drive the propeller.

## 4 Conclusion

The methodologies for modelling and simulation of hybrid power systems (PV/WECS) were provided in this study. The model was created with the MATLAB/SIMULINK software programme. The available power of the PV system is heavily contingent on solar radiation. To compensate for the PV system's deficiency, the PV module was connected to the wind turbine system. The designed system, as well as its control method, performs admirably. The presented model provides a useful tool for optimizing hybrid power performance. The elements of the basic and modified circuits are created using applicable formulae. Simulink library pieces are used to create simulation circuits. This MLI provides cost-effective, small-scale, high-energy conversion, and low THD solutions for PV and wind integration. Hybrid systems, according to the report, can improve energy supply stability and sustain a relatively consistent power supply from renewable resources for a specified operational zone. The investigation reveals a slew of possible benefits, including lower fuel usage as a result of lower exhaust gas emissions. Finally, based on the simulation results, the proposed system for marine applications can be implemented.

### Acknowledgment:

The first author, Professor and Dean Dr.T. Sasilatha, gratefully acknowledges the financial support obtained from the All India Council for Technical Education, India, under the Research Promotion Scheme.

### References:

- [1] F.D. Kanellosa, A. Anvari-Moghaddam, J.M. Guerrero, "A Cost-effective and Emission-aware Power Management System for Ships with Integrated Full Electric Propulsion", *Electric Power Systems Research*, vol. 150, pp. 63-75, 2017.
- [2] B. M. Guarnieri, M. Morandin, and A. Ferrari, "Electrifying Water Buses: A Case Study on Diesel-to-Electric Conversion in Venice," *IEEE Industry Applications Magazine*, vol. 24, no.1. pp. 71–83, 2017.
- [3] J. P. Trovão, F. Machado, P. G. Pereirinha, J. P. Trovão, F. Machado, and P. G. Pereirinha, "Hybrid electric excursion ships power supply system based on a multiple energy storage system," *IET Electr. Syst. Transp.*, vol. 6, no. 3, pp. 190–201, 2016.

- [4] A. Frances, A. Anvari-Moghaddam, E. Rodriguez-Diaz, J.C. Vasquez, J.M. Guerrero, J. Uceda, "Dynamic Assessment of COTS Converters based DC Integrated Power Systems in Electric Ships", IEEE Trans. Industrial Informatics, 2018. DOI:10.1109/TII.2018.2810323.
- [5] B. Karl and G. Aars, "Energy Savings in Coastal Fisheries," no. September, pp. 74–79, 2017. IEEE Electrification Magazine (Volume: 5, Issue: 3, Sept. 2017)
- [6] M. H. Nehrir, C. Wang, K. Strunz, H. Aki, R. Ramakumar, J. Bing, Z. Miao, and Z. Salameh (2011), "A Review of Hybrid Renewable/Alternative Energy Systems for Electric Power Generation: Configurations, Control, and Applications", IEEE Transactions on Sustainable Energy, Vol. 2, No. 4, pp392-403.
- [7] Sivachandran, P., Lakshmi, D., & Janani, R. (2015). Survey of maximum power point tracking techniques in solar PV system under partial shading conditions. ARPN Journal of Engineering and Applied Sciences, 10(1), pp. 256-264.
- [8] Vidhya, S., & Sasilatha, T. (2017). Performance analysis of ad-hoc on demand distance vector and energy power consumption AODV in wireless sensor networks. Journal of Computational and Theoretical Nanoscience, 14(3), 1265-1270.
- [9] Heier S. Grid integration of wind energy conversion system. Chichester: John Wiley & Sons, Ltd; 2006, ISBN 10: 0470868996.
- [10] Gnanavel, C., Rajavelan, M., Muthukumar, P., & Immanuel, T. B. (2018). A Performance Investigation of a Single Phase Multilevel Inverter Fed Nonlinear Loads for Solar PV Applications. International Journal of Engineering and Technology, 7(24), pp. 388-391.
- [11] Srujana, A., Lakshmi, D., Ravi, C. N., & Baskaran, S. (2021). Integrated Renewable Energy Sources for the minimization of Emission and Economic Operation of Power System. Int. J. of Aquatic Science, 12(3), 341-349.
- [12] Hui J, Bakhshai A, Jain PK. A hybrid wind-solar energy system: a new rectifier stage topology. In: Applied power electronics conference and exposition, February/2010, Palm Springs/USA. pp. 155–61.
- [13] Li Z, Wang P, Li Y, Gao F. A novel single-phase five-level inverter with coupled inductors. IEEE Trans Power Electron 2012;27(6):2716–25.
- [14] Balaji, S., & Sasilatha, T. (2019). Detection of denial of service attacks by domination graph application in wireless sensor networks. Cluster Computing, 22(6), 15121-15126.
- [15] Bagul, A. D., & Salameh, Z. M. (1996). Sizing of a stand-alone hybrid wind-photovoltaic system using a three-event probability density approximation. Solar Energy, 56, 323–335.
- [16] Vidhya, S., & Sasilatha, T. (2018). Secure data transfer using multi-layer security protocol with energy power consumption AODV in wireless sensor networks. Wireless Personal Communications, 103(4), 3055-3077.
- [17] Floricau D, Floricau E, Gateau G. New multilevel converters with coupled inductors: properties and control. IEEE Trans Ind Electron 2011;58(12):5344–51.
- [18] Sivachandran, P., Lakshmi, D., & Janani, R. (2015). Survey of maximum power point tracking techniques in solar PV system under partial shading conditions. ARPN Journal of Engineering and Applied Sciences, 10(1), 25
- [19] ]Roberto F. Coelho, Filipe Concer and Denizar C. Martins" A Study of basic DC-DC Converters applied in maximum power point Tracking, Brazilian Power Electronics Conference 2009
- [20] J. Iqbal and Z. H. Khan, "The potential role of renewable energy sources in robot's power system: A case study of Pakistan," *Renewable and Sustainable Energy Reviews (In Press)*, 2016.
- [21] R. K. Kharb, S. Shimi, S. Chatterji, and M. F. Ansari, "Modeling of solar PV module and maximum power point tracking using ANFIS," *Renewable and Sustainable Energy Reviews*, vol. 33, pp. 602-612, 2014
- [22] K. Lian, J. Jhang, and I. Tian, "A maximum power point tracking method based on perturb-and-observe combined with particle swarm optimization," *IEEE journal of photovoltaics*, vol. 4, pp. 626-633, 2014.
- [23] Y.-H. Liu, S.-C. Huang, J.-W. Huang, and W.-C. Liang, "A particle swarm optimization-based maximum power point tracking algorithm for PV systems operating under partially shaded conditions," *IEEE Transactions on Energy Conversion*, vol. 27, pp. 1027-1035, 2012.

- [24] S. K. Mahapatro, "Maximum Power Point Tracking (MPPT) Of Solar Cell Using Buck-Boost Converter," *International Journal of Engineering Research and Technology*, 2013.
- [25] N. Kodama, T. Matsuzaka, and N. Inomata, "Power variation control of a wind turbine generator using probabilistic optimal control, including feedforward control from wind speed," *Wind Eng.*, vol. 24, no. 1, pp. 13–23, Jan. 2000.
- [26] L. L. Freris, *Wind Energy Conversion Systems*. Englewood Cliffs, NJ: Prentice-Hall, 1990, pp. 182–184.
- [27] Q. Wang and L. Chang, "An intelligent maximum power extraction algorithm for inverter-based variable speed wind turbine systems," *IEEE Trans. Power Electron.*, vol. 19, no. 5, pp. 1242–1249, Sept. 2004.

#### **Contribution of Individual Authors to the Creation of a Scientific Article (Ghostwriting Policy)**

Dr. Priya, K. S. Kavitha Kumari reviewed the state of art and organized the section 1.

J. K. Vaijayanthimala and J. Padmapriya carried out the Modelling and Simulation for the PV/Wind System and also for the converter.

Dr. T. Sasilatha, Dr. D. Lakshmi, R. K. Padmashini carried out the Modelling and Simulation for the Hybrid System and the Multilevel Inverter.

#### **Creative Commons Attribution License 4.0 (Attribution 4.0 International, CC BY 4.0)**

This article is published under the terms of the Creative Commons Attribution License 4.0

[https://creativecommons.org/licenses/by/4.0/deed.en\\_US](https://creativecommons.org/licenses/by/4.0/deed.en_US)